Torsional vibration and sensitivity analysis of microcantilever in liquid

M. Soltani Tehrani[1] and R. Ghaderi[1,*]

[1]*Department of Mechanical Engineering, Shahrekord Branch, Islamic Azad University, Shahrekord, Iran*
*__Corresponding author__: reza.ghaderi@ymail.com

ABSTRACT Development of microsystems and ever-increasing advances of nanotechnology have resulted in growing applications of microcantilevers (MCs), including Atomic Force Microscopy (AFM). In AFM, transverse vibration of microfiber from a liquid medium results in resonance of unwanted hydrodynamic and electrostatic forces, which can be minimized by torsional mode. In the present study, the differential equation of the vibrational motion is extracted by acquiring the hydrodynamic force applied to MCs aiming to investigate the torsional vibration behavior of MCs in a liquid medium; and the extracted equation is solved to study the behavior of MCs in a liquid medium. Considering the significant effect of MC geometry on its torsional vibrations in a liquid medium, Sobol's variance-based sensitivity analysis method was utilized to investigate the effectiveness of MC geometry on torsional vibration. The sensitivity analysis results show that length and width have the most significant effects on the quality factor and the resonance frequency of MCs.

KEYWORDS Microcantilever; Torsional oscillation; Sensitivity analysis; Liquid

1. Introduction

The development and ever-increasing advances of microsystems in various aspects have led to growing applications of MCs. Today, MCs have a wide range of applications as in AFM (Alibakhshi et al., 2022; Tang et al., 2022; Yang et al., 2022), mass flow sensors (Kasambe et al., 2022; Panahi et al., 2021), accelerometers (Raj et al., 2021), and radiofrequency switches (Cheulkar et al., 2020; Thalluri et al., 2021). High speed, proper accuracy, and flexibility are the major advantages of MCs.

AFM is a major application of MCs, which are regarded as its heart. AFM performance in a liquid medium is essentially important, because biological samples can be examined in their physiological conditions only in this medium (Endo et al., 2018). The vibration of MCs in liquid medium in the vicinity of sample is always affected by the hydrodynamic force of the liquid, as well as the electrostatic interactions caused by surficial charges of the sample. Since the electrostatic interactions act perpendicular to the sample surface, the bending modes in tapping and contact modes is always affected by this force. Considering the fact that in torsional mode the AFM tip oscillates in the lateral direction, it is not affected by the electrostatic force. Therefore, the torsional vibration of MCs in a liquid medium is essentially important and it is necessary to examine its motions.

The torsional in AFM was used to extract the in plane mechanical properties of solid surfaces such as shear stiffness friction and other tribological properties in the air (Eichhorn and Dietz, 2022; Liu et al., 2018; Mumford et al., 2020; Tajeddin et al., 2021). Torsional mode in the modulation frequency was used for the first time by Kawai et al. (2005) in a vacuum medium. Later, Yurtsever et al. (2008) used this mode to image the sample surface in the air medium. In addition to the air medium, the torsional mode has been used in many studies to image the sample in a liquid medium (Abbasi and Karami Mohammadi, 2015; Huang and Su, 2004; Thalluri et al., 2021; Umemoto et al., 2020; Yu et al., 2020). Mullin and Hobbs (2008) used the torsional mode and amplitude modulation in the water medium. Yu et al. (2020) took high-resolution images in the water medium using torsional mode and frequency modulation.

Since vibrations in a liquid medium are affected by the hydrodynamic force of the liquid, dynamic modeling of the motion requires determining the liquid medium effect in form of an analytical expression. Aureli and Porfiri (2010) proposed the analytical expression of the hydrodynamic force function in torsional vibration, and investigated the nonlinear liquid effects caused by torsion in a relatively large amplitude. Green and Sader (2005) proposed the correction terms for the limited vibration amplitude in hydrodynamic function with torsional vibrations. Stokes (1851) assumed the hydraulic load as a torsional moment resisting against MCs motions and proposed an analytical expression for the hydrodynamic function.

Aiming to study the torsional vibrations of MCs in a liquid medium, this study used sensitivity analysis to investigate the effects of the MC geometry on the vibration parameters. Accordingly, the differential equation of the motion is extracted using analytical equations of hydrodynamic force in form of inertia and damping terms; and then the natural frequency and amplitude are extracted from the analytical motion of the equation in the liquid medium. Later, the effects of geometric dimensions on torsional vibrations are examined using Sobol's variance-based sensitivity analysis method.

DOI: 10.52292/j.laar.2024.1151
Received: August 18, 2022.
Accepted: May 3, 2023.
Recommended by Fabio Giannetti.

2. Dynamic modeling of MC in liquid

MCs used in microelectr omechanical systems undergo slight deformations. Therefore, not only Euler-Bernoulli beam model can be used to analyze their vibrations, but also the nonlinear terms of Navier-Stokes equations of their surrounding liquid can be disregarded. Accordingly, the slight deformations of MCs during the torsion can be used to obtain the differential equation of their motions. Considering Fig. 1 and the selected elements, the torsional moment generated at point x of the MC depends on the rotational moment ($T_d = T_d(x)e^{i\omega t}$), the resisting moment caused by the hydrodynamic force of the liquid (T_h), and torsional resistance of the MC. Considering the Free Body Diagram (Fig. 1), the equilibrium equation of the torsional moment in a viscous liquid medium can be indicated as follows:

$$\left(T_x + \frac{\partial T_x}{\partial x}dx\right) - T_x - T_d dx = \rho J \frac{\partial^2 \phi}{\partial x^2} \tag{1}$$

where ρ, J and ϕ represent the mass density of the base material, polar moment of the cross-section inertia, and rotational lift of MCs in y-z section respectively. Considering the equations governing the beams torsion, torsional moment at any given point can be expressed based on G (shear model) and K (torsion constant).

$$T_x = GK\frac{\partial \phi}{\partial x} \tag{2}$$

By inserting Eq. 2 into Eq. 1, and assuming that G and K are constant values, the differential equation of MCs vibrations in a liquid medium is worked out as follows:

$$GK\frac{\partial^2 \phi}{\partial x^2} - \rho J\frac{\partial^2 \phi}{\partial t^2} = T_d + T_h \tag{3}$$

Polar inertia moment (J) and constant torsional moment (K) can be calculated for rectangular sections using Eq. 4 and Eq. 5 (Sokolnikoff and Specht, 1956):

$$J = \frac{b^3 h + bh^3}{12} \tag{4}$$

$$K = \frac{2bh^3}{\overline{K}} \tag{5}$$

where $\overline{K}$ is extracted from Table 1.

The resisting moment generated by hydrodynamic force of the liquid (T_h) can be expressed based on torsional velocity and acceleration terms (Cai, 2013):

$$T_h\left(x, Re, \frac{h}{b}, t\right) = a_1\frac{\partial \phi(x,t)}{\partial t} + a_2\frac{\partial^2 \phi(x,t)}{\partial t^2} \tag{6}$$

where:

$$a_1 = \frac{\pi \rho_{liq} b^4 \omega}{8}\gamma\left(Re, \frac{h}{b}\right) \tag{7}$$

$$a_2 = \frac{\pi \rho_{liq} b^4}{8}\overline{\gamma}\left(Re, \frac{h}{b}\right) \tag{8}$$

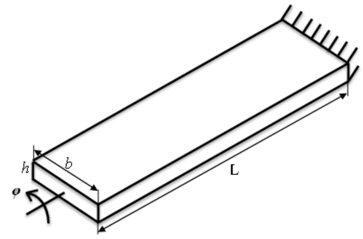

Figure 1: Schematic of MC.

Table 1: Material and geometry of the simulated MC.

h (µm)	b (µm)	L (µm)	E (Gpa)
22.3	90	400	110

where ρ_{liq}, Re, and ω represent density of liquid, Reynolds number, and excitation frequency respectively. Reynolds number is a dimensionless parameter defined by inertial force to viscous force ratio:

$$Re = \frac{\rho_{liq}\omega b^2}{4\eta} \tag{9}$$

where η is the kinematic viscosity. In Eq. 5 and Eq. 6, γ and $\overline{\gamma}$ are the real and imaginary parts of the hydrodynamic function. The hydrodynamic function is a dimensionless function that shows the effect of a viscous incompressible liquid on MC vibrations. Values of γ and $\overline{\gamma}$ in the hydrodynamic function can be expressed as follows (Cai, 2013).

$$\gamma = \left(0.05 + 0.24R^{-0.43}\right)\left[1.2 + \left(\frac{h}{b}\right)^{0.89}\right] \tag{10}$$

$$\overline{\gamma} = \left(Re^{-1} + 0.45R^{-0.5}\right)\left[0.75 + \frac{h}{b}\right] \tag{11}$$

By inserting Eq. 6 to Eq. 3 the differential equation of torsional vibration can be expressed as follows:

$$GK\frac{\partial^2 \phi}{\partial x^2} + (a_2 - \rho J)\frac{\partial^2 \phi}{\partial t^2} + a_1\frac{\partial \phi}{\partial t} = T_d e^{i\omega t} \tag{12}$$

Boundary conditions of the Differential Eq. 12 for MCs shown in Fig. 1, which is clamped at one end and free at the other end, is as follows:

$$\phi(0,t) = 0\ ;\ \frac{\partial \phi}{\partial x}(L,t) = 0 \tag{13}$$

The modal superposition method can be used to solve the Differential Eq. 12. In this method, the rotational lift of MCs can be defined as the sum of MC responses to each one of excitations in n oscillation modes.

$$\phi(x,t) = \sum_{n=1}^{\infty} C_n \varphi_n(x)e^{i\omega t} \tag{14}$$

In this equation, C_n represents the unknown coefficients and shows the weight of the effect of nth mode on the total

Table 2: Compare the resonance frequencies of MCs in the air and water ambient.

	Experimental Results (kHz) (Cai, 2013)	Analytical Results (kHz)	Difference with Experimental Results (kHz)
Air	1218.75	1219	0.017
Water	950.88	973.63	2.3

response. $\varphi_n(x)$ represents the shape function of MCs in torsional vibration, which can be defined considering the boundary condition of Eq. 13 as follows:

$$\varphi_n(x) = \sin\beta_n x \tag{15}$$

$$\beta_n = \frac{(2n-1)\pi}{L} \tag{16}$$

By inserting Eqs. 14 and 15 in Differential Eq. 12, multiplying $\varphi_n(x)$ by the two sides of the equation, and integrating along MCs, considering orthogonality of the shape functions, the rotational lift $\phi(x,t)$ can be expressed as follows:

$$\phi(x,t) = \sum_{n=1}^{\infty} \frac{\sin\beta_n x e^{j\omega t} \int_0^L T_d \varphi_n(x)\,dx}{L\left[GK\beta_n^2 - \omega^2(\rho J + a_2) + i\omega a_1\right]} \tag{17}$$

Since the tip rotational lift is essentially important in MCs, the dynamic torsion of the MC tip can be calculated by inserting $x = L$ in Eq. 17, assuming that the torsional moment is constant.

$$\phi(L,t) = \sum_{n=1}^{\infty} \frac{2(-1)^{n+1} T_d}{\beta_n L\sqrt{GK\beta_n^2 - \omega^2(\rho J + a_2)^2 + (\omega a_1)^2}} \tag{18}$$

where the MC is affected by harmonic excitations, the natural damping frequency can be expressed using damping ratio ξ and undamped resonance frequency of the n^{th} mode in viscous liquid medium (ω_{dn}) as follows:

$$\omega_{dn} = \beta_n \sqrt{\left(\frac{GK}{\rho J + a_2}\right)\left[1 - \left(\frac{2a_1}{\omega(\rho J + a_2)}\right)^2\right]^2} \tag{19}$$

Quality Factor is another important parameter in design of resonance frequency-based electromechanical systems. The quality factor in torsional vibration can be calculated based on the damping ratio as follows:

$$Q = \frac{1}{2\xi\sqrt{1-2\xi^2}} = \frac{\rho J + a_2}{C/\omega}\left[1 - \frac{1}{2}\left(\frac{C/\omega}{\rho J + a_2}\right)^2\right]^{-\frac{1}{2}} \tag{20}$$

3. Simulation of torsional vibration of MC in liquid

In order to simulate MC vibrations in a liquid medium, a MC with rectangular section, clamped at one end, is used as illustrated in Fig. 1.

The geometry of the simulated MC and specifications of the liquid medium are presented in Tables 2 and 3.

Table 3: Specifications of the liquid medium.

Glycerol percentage	0	20	40
Density (kg·m^3)	997	1058	1115
Dynamic viscosity (mPa)	0.89	1.75	4.04

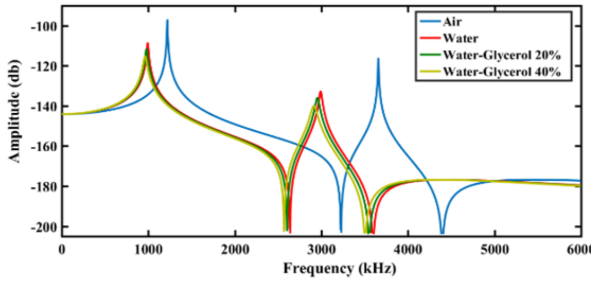

Figure 2: The effect of liquid medium on frequency response of MCs in the first two vibration modes.

The simulation results were verified using the practical tests on the MC vibrating in air and water mediums (Cai, 2013). Table 2 shows the proper compliance of the calculated resonance frequency and results of practical tests in air and water mediums.

When MC moves in the liquid medium, the liquid viscosity is regarded as a moving obstacle; furthermore, some liquids move along with MCs, which results in increased effective mass as the liquid mass is added to that of the beam. The increased mass, known as added mass, results in decreased resonance frequency of the MC. Figure 2 shows the effect of liquid medium on frequency response of MCs in the first two vibration modes. As expected, increasing the glycerol content solved in the water results in increased viscosity and density of the liquid medium, which eventually results in decreased resonance frequency and amplitude in both vibration modes. The simulation results show that decreased amplitude of vibration in the first oscillation mode is 97.5 % larger than that of the second oscillation mode when shifting from air medium to water medium; although the effect of this medium alteration on resonance frequency drop in the second oscillation mode is 98.6 % and it is greater than that of the first oscillation mode. Reynolds number is an important parameter in the study of MC vibration in a liquid medium. This number shows the effect of liquid viscosity on the inertial force. A greater Reynolds number in a vibrating motion shows that inertia has a more significant effect on the motion, compared with the hydrodynamic forces. The hydrodynamic force is usually difficult to calculate in a vibrating motion, and has to be estimated. Therefore, for MC vibration in a liquid medium, the in-

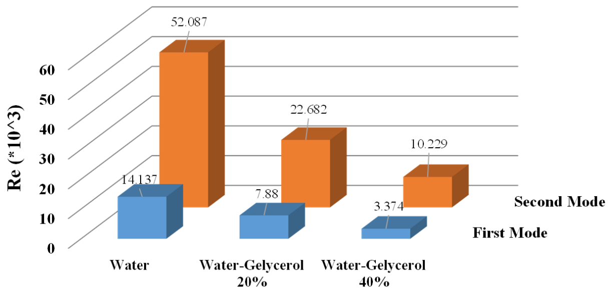

Figure 3: Effect of liquid concentration on Reynolds number.

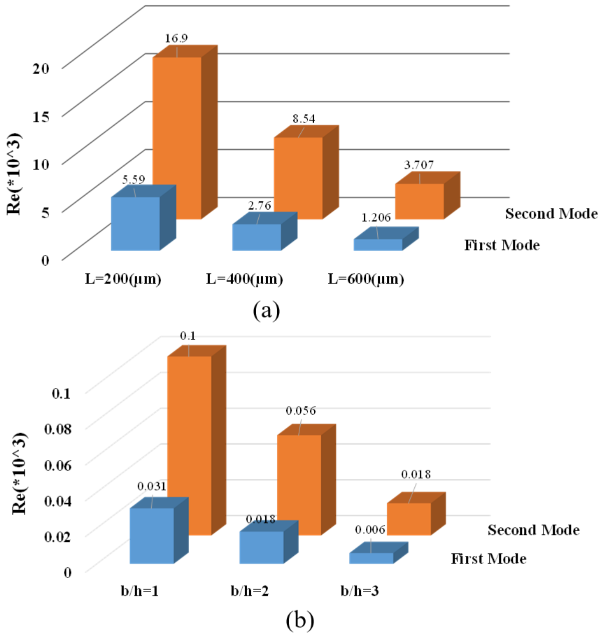

Figure 4: The effect of MC geometry on Reynolds number: (a) MC length, (b) aspect ratio b/h.

creased Reynolds number results in the decreased effect of the hydrodynamic force on vibration, and the dynamic simulation can be performed more accurately.

Increasing the glycerol content solved in the water results in increased viscosity and density of the liquid. Accordingly, the increased concentration of the liquid results in the increased hydrodynamic force, which leads to the decreased Reynolds number. The results in Fig. 3 show the effect of liquid concentration on Reynolds in the two first oscillation modes. As expected, the increased liquid concentration results in the reduced Reynolds number. Accordingly, the hydrodynamic force has a more significant effect than the inertial force. The results also show that in the second oscillation mode, the Reynolds number is greater in all three selected media, which is indicative of the reduced effect of hydrodynamic force on MC vibrations in the second oscillation mode. In addition to the medium, MC geometry has a significant effect on the Reynolds number. Fig. 4 shows the effect of MC geometry on Reynolds number. Results of Fig. 4a show that the increased length of MC has resulted in the decreased Reynold number in the first two oscillation modes, as a result of which, the effect of hydrodynamic force on MC vibration is more significant than that of the inertial force. Results of Fig. 4b show that the square section has the largest Reynolds number. Accordingly, the dynamic force has the minimum effect on this section in both torsional vibration modes, and the dynamic simulation results of this section are expected to be more accurate than those of the rectangular section. Vibration parameters, including resonance frequency, depend on different variables such as geometrical aspects of MCs; and the effect of this parameter on the resonance frequency must be examined continuously. Therefore, it is necessary to use sensitivity analysis methods, which, like Sobol's method, not only help us examine the effect of geometrical aspects on resonance frequency, but also make it possible to calculate the effect of each one of these parameters on resonance frequency. The Sobol method is efficient for analysis of complex models and can conduct absolute sensitivity analysis of the inputs. Additionally, this method can determine the sensitivity of the MC deformation output to input variables.

Figure 5 shows the effect of MC geometry on torsional resonance frequency in the first two oscillation modes. Figure 5a shows the effect of the MC length on resonance frequency. Considering the results, it can be concluded that increasing the MC length results in decreased resonance frequency in the first two oscillation modes in a liquid medium. The results also show that the resonance frequency drop caused by the increased length is more significant in the second oscillation mode than the first oscillation mode. The increased MC thickness results in the increased MC stiffness, and eventually in the increased resonance frequency, as confirmed by results of Fig. 5b. The results show that MC thickness has a more significant effect on resonance frequency in the second oscillation mode. Results of Fig. 5c show that the MC resonance frequency in a liquid medium is minimized in the first and second modes for widths of 36.3 and 38.2 μm, respectively. Figure 6 shows the effects of different geometrical aspects of MCs on resonance frequency in the two first oscillation modes, extracted from Sobol's variance-based sensitivity analysis method. As shown in this figure, the MC width and thickness have the most significant effects on resonance frequency during the first and second oscillation modes in a liquid medium, respectively. These parameters are the most important parameters in geometrical design of MCs. In order to reduce the effect of liquid medium on MC vibration, the geometric aspects of MCs must be selected in such a way that the quality factor is minimized. Sobol's variance-based sensitivity analysis method can be used to investigate the effect of the geometric aspects of MCs on quality factor and find out the optimal geometric aspects.

Figure 7 shows the effect of the geometric aspects of MC on quality factor. Results of Figs. 7a and 7b show that the increased length and width of MCs results in the decreased quality factor; and eventually the liquid medium will have a less significant effect on torsional vibration of MCs in both oscillation modes. Unlike length and width,

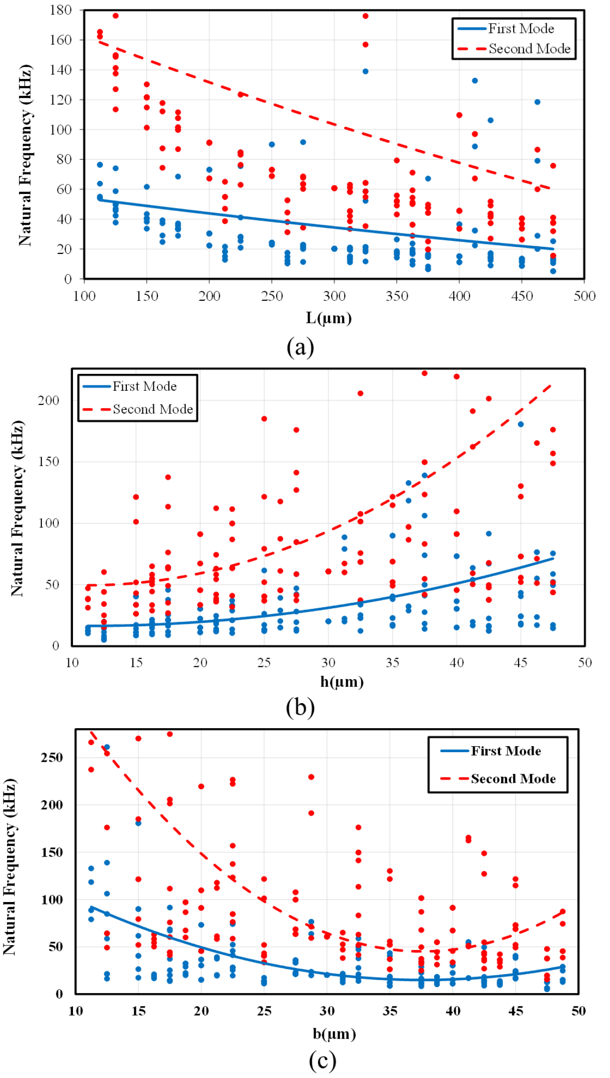

Figure 5: The effect of MC geometry on torsional resonance frequency in the first two oscillation modes: (a) L, (b) h, (c) b.

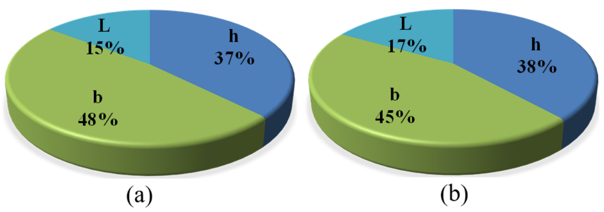

Figure 6: Level of influence of MC geometrical parameter on resonance frequency, (a) first mode, (b) second mode.

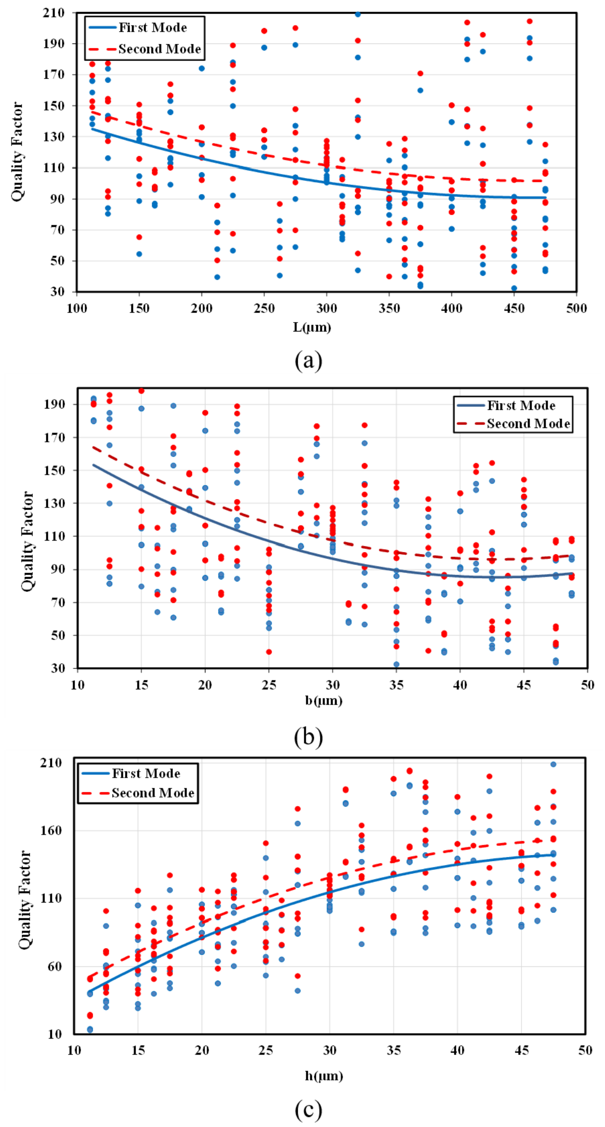

Figure 7: The effect of the MC geometric parameters on quality factor, (a) L, (b) b, (c) h.

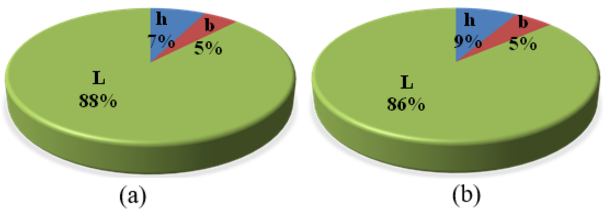

Figure 8: Level of influence of MC geometric parameters on quality factor, (a) first mode, (b) second mode.

the increased thickness of MCs results in the intensified effect of quality factor in both oscillation modes as shown by the results of Fig. 7c. Therefore, it can be concluded that reducing the liquid medium effect on vibration of MCs requires maximizing the length and width of the MC and minimizing its thickness. Figure 8 shows the effect of geometric aspects of MCs in the two fist oscillation modes. The results show that the MC length has the most significant effect on quality factor in both vibration modes.

4. Conclusion

MCs are amongst the main components of the microelectromechanical systems, which have become increasingly popular due to development of such systems. Since the effects of hydrodynamic and electrostatic forces are reduced in torsional vibrations, the present study investigated MC vibrations in a liquid medium. Sobol's variance-based sensitivity analysis method was used to examine the effect of geometric aspects on vibrations. The simulation and sensitivity analysis results for MCs in a liquid medium showed that:

1. Considering the fact that the Reynolds number of the second oscillation mode is greater than that of the first mode, the hydrodynamic force has a less significant effect on torsional vibrations in this mode.
2. Square section has a greater Reynolds number; therefore, the hydrodynamic force effect on torsional vibrations is minimized for this section.
3. The sensitivity analysis results suggest that the increased length and thickness of MCs results in decreased resonance frequency in both modes in a liquid medium.
4. Results of sensitivity analysis on quality factor show that MC length has the most significant effect on this parameter in the two first oscillation modes.

References

Abbasi, M. and Karami Mohammadi, A. (2015). Study of the sensitivity and resonant frequency of the torsional modes of an AFM cantilever with a sidewall probe based on a nonlocal elasticity theory. *Microsc. Res. Tech.*, 78(5):408–415.

Alibakhshi, A., Dastjerdi, S., Malikan, M., and Eremeyev, V. A. (2022). Nonlinear free and forced vibrations of a dielectric elastomer-based microcantilever for atomic force microscopy. *Contin. Mech. Thermodyn.*, pages 1–18.

Aureli, M. and Porfiri, M. (2010). Low frequency and large amplitude oscillations of cantilevers in viscous fluids. *Appl. Phys. Lett.*, 96(16).

Cai, T. (2013). *Theoretical analysis of torsionally vibrating microcantilevers for chemical sensor applications in viscous liquids*. PhD thesis, Marquette University, USA.

Cheulkar, L. N., Sawant, V. B., and Mohite, S. S. (2020). Evaluating performance of thermally curled microcantilever RF MEMS switches. *Mater. Today Proc.*, 27:12–18.

Eichhorn, A. L. and Dietz, C. (2022). Torsional and lateral eigenmode oscillations for atomic resolution imaging of HOPG in air under ambient conditions. *Sci. Rep.*, 12(1):8981.

Endo, D., Yabuno, H., Yamamoto, Y., and Matsumoto, S. (2018). Mass sensing in a liquid environment using nonlinear self-excited coupled-microcantilevers. *J. Microelectromechanical Syst.*, 27(5):774–779.

Green, C. P. and Sader, J. E. (2005). Frequency response of cantilever beams immersed in viscous fluids near a solid surface with applications to the atomic force microscope. *J. Appl. Phys.*, 98(11):114913.

Huang, L. and Su, C. (2004). A torsional resonance mode AFM for in-plane tip surface interactions. *Ultramicroscopy*, 100(3-4):277–285.

Kasambe, P. V., S. Bhole, K., Bage, A. A., Raykar, N. R., and Bhoir, D. V. (2022). Analytical modeling and numerical investigation of a variable width piezoresistive multilayer polymer micro-cantilever air flow sensor. *Adv. Mater. Process. Technol.*, 8(4):4365–4383.

Kawai, S., Kitamura, S.-i., Kobayashi, D., and Kawakatsu, H. (2005). Dynamic lateral force microscopy with true atomic resolution. *Appl. Phys. Lett.*, 87(17):173105.

Liu, L., Xu, J., Zhang, R., Wu, S., Hu, X., and Hu, X. (2018). Three-dimensional atomic force microscopy for sidewall imaging using torsional resonance mode. *Scanning*, 2018:1–8.

Mullin, N. and Hobbs, J. (2008). Torsional resonance atomic force microscopy in water. *Appl. Phys. Lett.*, 92(5):053103.

Mumford, S., Paul, T., Lee, S. H., Yacoby, A., and Kapitulnik, A. (2020). A cantilever torque magnetometry method for the measurement of Hall conductivity of highly resistive samples. *Rev. Sci. Instrum.*, 91(4):045001.

Panahi, A., Ghasemi, P., Sabour, M. H., Magierowski, S., and Ghafar-Zadeh, E. (2021). Design and modeling of a new MEMS capacitive microcantilever sensor for gas flow monitoring. *IEEE Can. J. Electr. Comput. Eng.*, 44(4):467–479.

Raj, Y., Shukla, K., Datta, T., and Sen, M. (2021). Micro cantilever-based optical gravimeter. *IEEE Sens. J.*, 21(13):14759–14766.

Sokolnikoff, I. and Specht, R. (1956). *Mathematical Theory of Elasticity*. McGraw-Hill, New York, USA.

Stokes, G. G. (1851). On the effect of internal friction of fluids on the motion of pendulums. *Trans. Cambridge Philos. Soc.*, 9(2):8–106.

Tajeddin, A., Mustafaoglu, N., and Yapici, M. K. (2021). On-chip measurement of pH using a microcantilever: A biomimetic design approach. In *2021 Symp. Des. Test, Integr. Packag. MEMS MOEMS*, pages 01–05. IEEE.

Tang, X., Fan, G., Zhang, H., Dai, X., Hu, Y., Zhang, Z., and Li, Y. (2022). An integrated optical waveguide micro-cantilever system for chip-based AFM. *J. Microsc.*, 285(2):112–116.

Thalluri, L., Kumar, K., Sekhar, K., Babu, B., Kiran, S., and Guha, K. (2021). Damping analysis to improve the performance of shunt capacitive RF MEMS switch. *Facta Univ. - Ser. Electron. Energ.*, 34(3):381–392.

Umemoto, M., Kawamura, R., Yoshikawa, H. Y., Nakabayashi, S., and Kobayashi, N. (2020). Simultaneous atomic-resolution flexural and torsional imaging in liquid by frequency modulation atomic force microscopy. *Jpn. J. Appl. Phys.*, 59(SI):SIII01.

Yang, R., Ogura, I., Jiang, Z., An, L., Ashida, K., and Yabuno, H. (2022). Nanoscale cutting using self-excited microcantilever. *Sci. Rep.*, 12(1):618.

Yu, J.-R., Chou, H.-C., Yang, C.-W., Liao, W.-S., Hwang, I.-S., and Chen, C. (2020). A horizontal-type scanning near-field optical microscope with torsional mode operation toward high-resolution and non-destructive imaging of soft materials. *Rev. Sci. Instrum.*, 91(7):073703.

Yurtsever, A., Gigler, A. M., and Stark, R. W. (2008). Frequency modulation torsional resonance mode AFM on chlorite (001). *J. Phys. Conf. Ser.*, 100(5):052033.